Microfluid Nanofluid
DOI 10.1007/s10404-012-1049-9

RESEARCH PAPER

# Fabrication and in situ characterization of microcapsules in a microfluidic system

**T. X. Chu · A.-V. Salsac · D. Barthès-Biesel · L. Griscom · F. Edwards-Lévy · E. Leclerc**



Received: 7 May 2012 / Accepted: 30 July 2012


**Abstract** We have designed a microfluidic system that enables both the fabrication of calibrated capsules and the in situ characterization of their mechanical properties. The fabrication setup consists of a double flow-focusing system. A human serum albumin aqueous solution is introduced in the central channel of a first Y-junction. Intercepted by the lateral flows of a hydrophobic phase, it is dispersed into microdroplets. A cross-linking agent is then introduced at a second Y-junction allowing a membrane to form around the droplets. The time of cross-linking is controlled by the length of a wavy channel located downstream of the second junction. A cylindrical microchannel finally enables to deform and characterize the capsules thus formed. The mechanical properties of the capsule membrane are obtained by inverse analysis. The results show that the drop size increases with the flow rate ratio between the central and lateral channels. The mean shear modulus of the capsules fabricated after 23 s of cross-linking is of the order of the surface tension between the two phases indicating that a reaction time of 23 s is too short for an elastic membrane to form around the droplet. When the cross-linking time is increased to 60 s, the microcapsules surface is wrinkled, thus confirming that a solid membrane is formed around the drop. The mean shear modulus of the capsule membrane increases with the cross-linking time, which is in agreement with our previous chemical results and proves that a fine control of the mechanical properties is possible by choosing adequately the control parameters of the system.

**Keywords** Flow-focusing microfluidic system · Capsule fabrication · Capsule characterization · Interfacial cross-linking · Two-phase flow · Serum albumin

T. X. Chu · A.-V. Salsac · D. Barthès-Biesel · E. Leclerc (✉)
UMR CNRS 7338, Biomécanique et Bioingénierie,
Université de Technologie de Compiègne,
Compiègne Cedex, France
e-mail: eric.leclerc@utc.fr

D. Barthès-Biesel
e-mail: dbb@utc.fr

L. Griscom
UMR CNRS 8069, SATIE/BIOMIS,
ENS de Cachan antenne de Bretagne, Bruz, France

F. Edwards-Lévy
UMR CNRS 7312, Institut de Chimie Moléculaire de Reims,
Faculté de Pharmacie, Université de Reims
Champagne-Ardenne, Reims, France

## 1 Introduction

Capsules consisting of a liquid droplet enclosed within a thin deformable membrane are commonly used in the pharmaceutical (Kissel et al. 2006), cosmetic (Miyazawa et al. 2000) and food industries (Gibbs et al. 1999). Encapsulation allows the protection of the internal substance and its release by controlling the membrane physical properties, porosity and break-up.

Most conventional encapsulation processes consist of two successive steps: fabrication of droplets and formation of the membrane around the droplet. Droplets may be formed by emulsification through mechanical agitation (Edwards-Lévy et al. 1993; Poux and Canselier 2004) or by extrusion and jet break-up (Gautier et al. 2011). The membrane may be created for example by protein cross-linking (Edwards-Lévy et al. 1993; Callewaert et al. 2009), complex coacervation (De Kruif et al. 2004) or solvent evaporation (Sawalha et al. 2011). These different conventional techniques are largely used in industrial applications because they allow the production of large quantities





Journal : Large 10404 | Dispatch : 4-9-2012 | Pages : 9
Article No. : 1049 | ☐ LE | ☐ TYPESET
MS Code : mfnf-120507 | ☑ CP | ☑ DISK

of capsules. However, they do not allow the fabrication of monodispersed capsules with homogeneous mechanical properties.

Microfluidic techniques have been recently proposed (Thorsen et al. 2001) to improve the homogeneity of microcapsule size and physical properties. Indeed, microfluidic devices allow the fabrication of calibrated drops through the injection of a disperse phase into a flowing immiscible continuous phase. Monodispersed microdrops can be produced using a T-junction microchip (Garstecki et al. 2006), a flow-focusing microchip (Yobas et al. 2006) or a microfluidic system based on co-axial cylindrical channels (Liu et al. 2009). The encapsulation process can be performed outside (outline) or inside (online) the system. For outline encapsulation, monodisperse microdrops formed at a cross-junction are collected in a reservoir containing a cross-linking solution (Huang et al. 2007; Yeh et al. 2009). The mechanical properties of the microcapsule membranes are not quite uniform because the droplets do not all have the same residence time in the reservoir. For online microcapsule fabrication, drops that are formed at the first cross-junction are stabilized at a second cross-junction, through which a cross-linking phase is injected. A downstream channel allows the control of the polymerization time of the microcapsules before collection (Zhang et al. 2006). The fabricated microcapsules then have a controlled membrane thickness and a controlled size.

Another issue is the determination of the membrane mechanical properties for which different methods have been proposed depending on the capsule size (Mercadé-Prieto and Zhang 2012). For example, a millimetric capsule can be compressed between two parallel plates and the compression force is then measured as a function of the plate separation (Carin et al. 2003). For micrometric capsules, a micropipette is used to measure the capsule length aspirated into the pipette under a given depression (Needham and Zhelev 1996). It is also possible to deform the microcapsule under a known force by means of an atomic force microscope (Fery and Weinkamer 2007). The latter techniques are difficult to implement because of the small capsule size. Conversely, the membrane elastic modulus of a microcapsule population can be characterized by flowing a capsule suspension in a small channel, measuring the deformed profile and the velocity of the particles and analyzing the results by means of a numerical model of the mechanical process (Lefebvre et al. 2008; Chu et al. 2011).

The objective of this paper was to show that it is possible to fabricate microcapsules in a microfluidic system under controlled conditions. The mechanical properties of the resulting capsules are then measured on-line with the aforementioned microfluidic technique. We have designed a microfluidic system that combines a double flow-focusing setup for capsule fabrication, ending with a microchannel for the characterization of the microcapsule mechanical properties. Thanks to this device, microdroplets are created at a first Y-junction. A membrane is formed around the microdroplets by reticulation through the injection of a cross-linking agent at a second Y-junction. The cross-linking time is controlled by the length of the channel present after the second Y-junction. After cross-linking, the microcapsules are flowed in a glass capillary tube located downstream and embedded in the PDMS. The tube diameter is of the same order as the capsule characteristic size, so that the microcapsules deform under the shear stress. The microcapsule mechanical properties are characterized using the inverse method previously described. In this paper, we study the formation of microcapsules containing an aqueous solution enclosed in a network of cross-linked serum albumin (Edwards-Lévy 2011). The continuous phase is a hydrophobic liquid ester (Dragoxat) used in the cosmetic and pharmaceutical domains (Hurteaux et al. 2005). The cross-linking agent is an acyl dichloride, the terephtaloyl chloride.

In Sect. 2, we present the fluid phases and the principle of microencapsulation using interfacial cross-linking of a protein, the microsystem design and fabrication technique, and the different aspects of the experimental procedure. The size of the capsules formed in the microsystem as well as the measured value of their membrane mechanical properties are detailed in Sect. 3. We finally discuss the process and conclude in Sect. 4.

## 2 Materials and methods

### 2.1 Fluid phases for the interfacial cross-linking of serum albumin

Interfacial cross-linking of proteins has been extensively studied by M.-C. Lévy and co-workers for the production of biocompatible and biodegradable microcapsules with tailored properties for pharmaceutical or cosmetical purposes (Edwards-Lévy et al. 1993, 1994, 2011; Lévy et al. 1991; Andry et al. 1996). The method involves an acylation reaction between the functional reactive groups of the protein present in the aqueous droplets of a water-in-oil emulsion and a bifunctional acylating reagent, such as an acyl dichloride, added to the external organic phase. During the process, free amino groups, hydroxyl groups and acid groups of the protein become linked through amide bonds, ester bonds and anhydride bonds, respectively. Acylation takes place at the interface, and a membrane, made of a cross-linked protein network, is formed.

The reaction parameters, i.e. concentration of the protein and concentration of the cross-linking agent, reaction time and reaction pH, influence the membrane cross-linking







Journal : Large 10404 Dispatch : 4-9-2012 Pages : 9
Article No. : 1049 LE TYPESET
MS Code : mfnf-120507 CP DISK

degree: they thus affect the degradation properties and mechanical properties of the microcapsules. When the process is conducted in an emulsion system, the emulsification parameters, i.e. stirring speed, viscosities of the two phases, nature and concentration of the surfactant, influence the mean size and the granulometric profiles of the microcapsules. In the present study, the constitutive protein is human serum albumin (HSA). The disperse phase consists of a 20 % HSA solution prepared in a phosphate buffer pH 9.8 to favor a rapid acylation. Its viscosity is $\mu = 3.31$ mPa s at 25 °C. The continuous phase is a biocompatible liquid ester, 2-ethylhexyl 2-ethylhexanoate (Dragoxat, Symrise). It is a hydrophobic fluid with viscosity $\mu = 3.5$ mPa s at 25 °C. It has been chosen as the external phase because usual organic volatile solvents like cyclohexane are deleterious to the polydimethylsiloxane (PDMS) used to fabricate the microsystem. The surface tension between the Dragoxat and the HSA solution is $\gamma = 0.006$ N/m (Tensiometer Kruss DSA10 Mk2).

The cross-linking phase contains terephthaloyl chloride (TC), an acyl dichloride, dissolved in Dragoxat: it cross-links HSA at the surface of the aqueous droplets formed in the microsystem. It is obtained by mixing 0.25 mg of TC powder in 10 ml of Dragoxat and stirring for 2 h with a magnetic stirrer. In order to avoid clogging of the microfluidic channel, the undissolved TC remaining in the solution after mixing is eliminated using a filter of size $\sim 1$ µm.

## 2.2 Microsystem design and fabrication

We have designed a microsystem with a double flow-focusing junction as illustrated in Fig. 1. The HSA solution is injected in the central channel (1). The Dragoxat is injected in the two lateral channels (2) making a 80° angle with channel 1 [the angle value was selected from our previous work (He et al. 2010); it contributes to prevent contact between the HSA solution and the wall]. Droplets are formed at the first junction between channel 1 and channels 2. Compared to a T-junction this flow focusing configuration limits the possible adsorption of the central droplet phase on the walls. After the junction, the central channel has the same dimensions as channel 1. The cross-linking phase, i.e. the solution of terephthaloyl chloride in Dragoxat, is injected at the second junction through the two lateral channels (3), which also make a 80° angle with the central channel. The droplet, surrounded by the cross-linking phase, then flows in channel 4, the waviness of which favors mixing and enables a homogeneous concentration of the cross-linking agent. The cross-linking time is controlled by the length and cross-section of channel 4. Its cross-section is larger than that of channel 1 to slow the microcapsules down. A cylindrical channel of internal radius $R$ is inserted inside channel 5 for microcapsule characterization. Finally, the microcapsules are collected in reservoir 6.

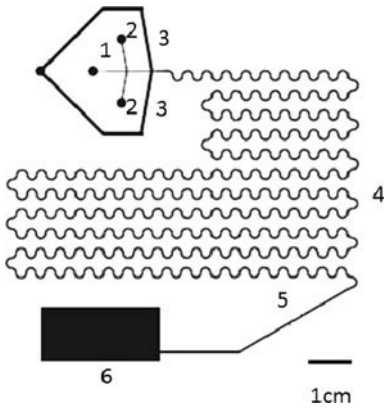


**Fig. 1** Microfluidic system for microcapsule fabrication and characterization

The main parameters for droplet fabrication are the channel cross-section dimensions and the flow rates of central and lateral fluids.

The procedure of fabrication of the PDMS microsystem is classical. The mould master, which consists of a SU8 photoresist patterned on a Silicon wafer, is manufactured by photolithography. Briefly, the SU8 photoresist is deposited on a silicon wafer by spin coating. Successive spin coating applications of the SU-8 photoresist allow the fabrication of multi-height microfluidic channels through mask alignment and multiple UV exposures (multiple UV lithographies were used to create the higher height $h_4$ in the channel sections 4, 5 and 6, see Table 1 to increase cross-linking time). After exposure, the system is immersed and agitated in a 1-Methoxy-2-propyl acetate developer solution to dissolve the unexposed parts.

A mixture of PDMS with curing agent (10:1 mass ratio) is then poured onto the mold master. The system is degassed to remove the air bubbles and heated in the oven at 70 °C for 2 h. The PDMS mould is peeled off the master and five holes are drilled into it for the injection of the solutions and collection of the capsules. The PDMS is bonded onto a glass substrate using plasma treatment to close the channels. The system is used a few days after fabrication to allow the PDMS to retrieve its hydrophobicity.

Three chips have been designed with width, depth and length of channel $i$ denoted $W_i$, $h_i$ and $L_i$, respectively. The geometric parameters of the dry chips under vacuum are given in Table 1.

## 2.3 Experimental observation technique and PDMS swelling problem

To visualize the experiments, the microsystem is placed under a microscope (Leica, Germany). Images are recorded





Journal : Large 10404 | Dispatch : 4-9-2012 | Pages : 9
Article No. : 1049 | LE | TYPESET
MS Code : mfnf-120507 | CP | DISK

**Table 1** Dry chip geometric parameters

| System | $W_1$ (μm) | $W_2$ (μm) | $h_1$ (μm) | $W_4$ (μm) | $h_4$ (μm) | $L_4$ (cm) |
|---|---|---|---|---|---|---|
| 1 | 103 | 215 | 115 | | | |
| 2 | 103 | 215 | 115 | 300 | 200 | 68 |
| 3 | 109 | 110 | 88 | 290 | 320 | 100 |

System 1 is devoid of a wavy channel

using a high-speed camera (Photron, Fastcam SA3), which has a nominal frame rate of 2000 frames/s. Visualizations are performed under the 20 × magnification. The image calibration is achieved using a Malassez (Marienfeld, Germany) 50 × 50 μm$^2$. The calibration indicates that 42 pixels correspond to 50 μm.

Experimental observations show that the channel width decreases when Dragoxat is injected into the microsystem (Fig. 2a, b). PDMS swelling has previously been observed in the case of contact with ethyl acetate (Ng Lee et al. 2003; Nguyen et al. 1999) and silicone oil (Anna et al. 2003). Using the image calibration, we estimate the channel width before and after Dragoxat injection. For each experimental setup, we measure the modified width of the central, lateral and wavy channels, $W_1', W_2'$ and $W_4'$, respectively. As for the height of the channels, no direct measurement can be made. We have therefore assumed the modified depth of the central channel to be $h_1' = h_1 - (W_1 - W_1')/2$, since swelling occurs only along one side of the channel (the bottom surface is the glass substrate). Similarly, the modified depth of the wavy channel is assumed to be $h_4' = h_4 - (W_4 - W_4')/2$.

## 2.4 Experimental procedure

In order to study the droplet generation process, channel 3 is first closed in microchip 1.

At first, the dragoxat is injected into the lateral channels 2 using a two-channel syringe pump (KD system) leading to equal flow rates $Q_2$ in each branch. Then the serum albumin solution is injected into channel 1 at a flow rate $Q_1$ using a second syringe pump.

To obtain the cross section of the drop in its axial plane, the microscope is focused on the middle plane of the channel. The drop size is characterized by the droplet length $L_g$ in the central channel downstream of the junction (Fig. 3).

To produce microcapsules, we open channel 3 and first inject the pure Dragoxat solution with equal flow rates $Q_3$ in each branch to stabilize the flow. Then, the cross-linking phase is injected with the same flow rates $Q_3$. As the cross-section of channel 4 is larger than that of channel 1, the microcapsules take a spherical shape from the second junction onwards. The microcapsule size is equal to the microdroplet size measured after the first junction, as their volume only differs by a thin membrane. The radius of the undeformed (i.e. spherical) microcapsule $a$ is obtained from its volume. The volume is calculated from the deformed shape of Fig. 3, assuming the capsule to be an ellipsoid with diameters $L_g, W_1', h_1'$. The membrane formation occurs while the microdroplet is traveling inside the wavy channel. The microdroplet diameter is of order 200 μm, while the cross dimension of the channel is of order 300 μm. The velocity of a centered microdroplet and later of the microcapsule will be slightly larger than the mean flow velocity, but it is difficult to determine with precision. Consequently, the order of magnitude of the cross-linking time $t_r$ is evaluated from the mean flow velocity in the wavy channel.

$$t_r = L_4 \frac{W_4' h_4'}{Q_1 + 2Q_2 + 2Q_3} \quad (1)$$

In order to measure the elasticity of the capsule membrane, a glass cylindrical microchannel with internal radius $R = 100$ μm is inserted into channel 5 to deform the microcapsules. The camera and microscope are positioned on channel 5 to measure simultaneously the velocity and the deformed profile of the flowing capsules. These results are

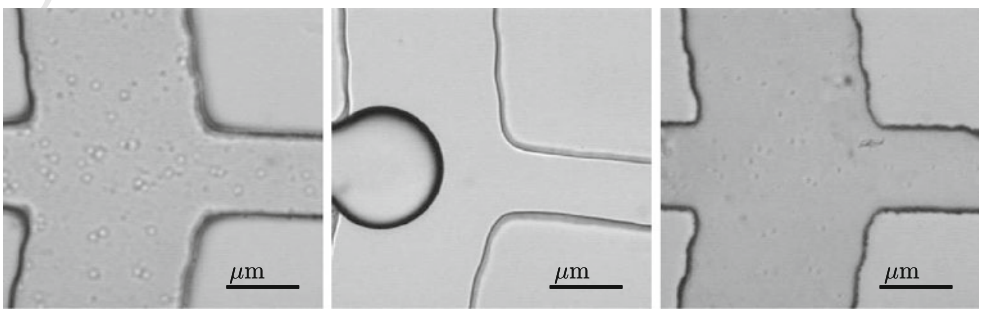


**Fig. 2** Decrease in the channel width of microsystem 1 in presence of Dragoxat. **a** Microsystem under vacuum; **b** microsystem in presence of Dragoxat and **c** microsystem after dragoxat removal and channel cleaning





Journal : Large 10404 Dispatch : 4-9-2012 Pages : 9
Article No. : 1049 LE TYPESET
MS Code : mfnf-120507 CP DISK

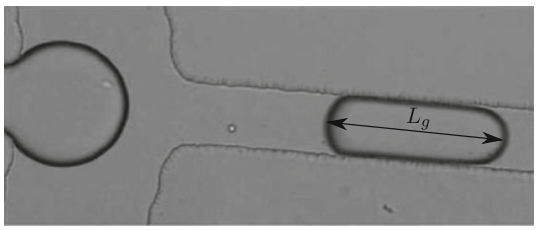


**Fig. 3** Formation of the drop at the first junction

then analyzed with the procedure described in our previous works (Lefebvre et al. 2008; Chu et al. 2011) and briefly summarized below in the membrane characterization section. In practice, we had to wait for a few minutes to achieve a stable flow configuration for the microdroplet formation and 20 min more to achieve stable microcapsules formation.

## 3 Results

### 3.1 Control of the capsule size

We first close channel 3 to study the variation of the drop size as a function of the flow rate ratio between the central and lateral channels. The results measured in chips 1 and 2 are shown in Fig. 4. The normalized drop length $L_g W_2'/h_1' W_1'$ increases linearly with the flow rate ratio $Q_1/Q_2$. It follows the linear regression curve

$$\frac{L_g W_2'}{h_1' W_1'} \approx 7\frac{Q_1}{Q_2} + 4.9 \qquad (2)$$

In a previous study conducted with the same fluid couple, we had already shown the linear dependency of the normalized drop length with the flow rate ratio (He et al. 2010). The slope of the regression had, however, been found to be about half the present value. A few reasons may account for the discrepancy. One of them is the swelling phenomenon, which had not been taken into account in the previous study. Since then, we have also calibrated the actual flow rate values provided by the pumps to account for the time fluctuations. Finally, we have improved the image analysis by enhancing the luminosity and contrast using a more sensitive camera and new microscope objectives. Even though we have optimized the quality of the measurements, a dispersion is still observed (Fig. 4). During the microdroplet formation, we calculated a standard deviation of 7 % on the measured droplet length $L_g$. In addition, resulting from independent experiments the total standard deviation was calculated at 20 %.

When the cross-linking phase is injected through channel 3, it is verified that it has no influence on the drop formation in the upstream bifurcation. In particular, the drop size does not change.

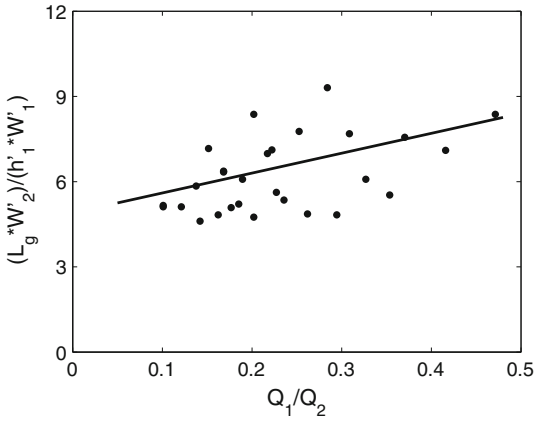


**Fig. 4** Variation of the normalized droplet length with the flow rate ratio $Q_1/Q_2$ in microsystems 1 and 2

### 3.2 Residence time and polymerization

The cross-linking degree is a function of the residence time of the capsules in the wavy channel (channel 4). The residence time can be modified by varying either the flow rate in the channel or the channel length. Different flow conditions have been studied. Using chip 2, we have set $Q_2$ to 33 μL/min and $Q_3$ to 12.5 μL/min, and varied $Q_1$ from 7 to 15 μL/min to change the capsule size. These conditions lead to a cross-linking time of order $t_r = 23$ s. A typical capsule deformed profile in channel 5 is shown in Fig. 5a. Then using chip 3 with the longer wavy channel, we have first set $Q_2 = 25$ μL/min, $Q_3 = 17$ μL/min, and varied $Q_1$ from 6 to 9.2 μL/min. The cross-linking time is found to be of order $t_r = 60$ s. Otherwise, imposing $Q_2 = 22$ μL/min, $Q_3 = 14$ μL/min, and varying $Q_1$ from 5 to 8 μL/min, we have obtained a cross-linking time of order $t_r = 70$ s. The corresponding capsule profile are shown in Fig. 5b, c, respectively.

We note that, whereas the capsule profile in Fig. 5a, is smooth, the other two profiles (Fig. 5b, c) are wrinkled. The very presence of the wrinkles proves that a thin solid membrane has been formed and that the capsule has not been gelled throughout. Indeed, a liquid-liquid interface is always smooth due to the surface tension. The folds are a consequence of the compression of the membrane in the azimuthal direction, which leads to buckling. This phenomenon has been also observed in a numerical model of the flow of an initially spherical capsule in a cylindrical tube (Hu et al. 2012). We conclude that for a long enough residence time in channel 4, the cross-linking of the membrane has time to occur.

### 3.3 Membrane characterization

An inverse method is used to deduce the capsule shear modulus from the experimental measurements on capsules





Journal : Large 10404 | Dispatch : 4-9-2012 | Pages : 9
Article No. : 1049 | LE | TYPESET
MS Code : mfnf-120507 | CP | DISK

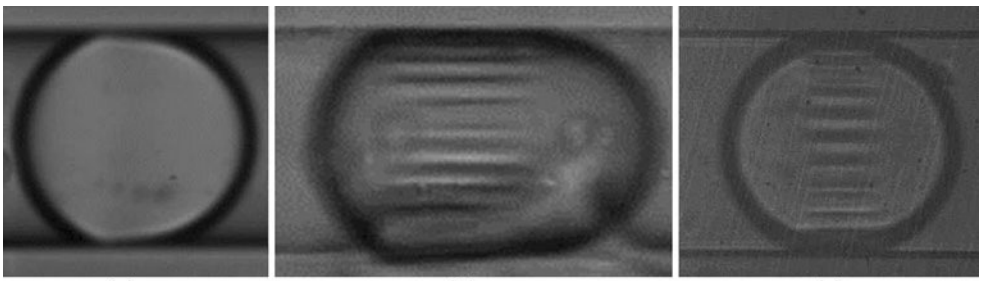


**Fig. 5** Pictures of microcapsules fabricated in situ and flowing down the cylindrical channel. **a** $t_r = 23$ s, $a/R = 1.08$; **b** $t_r = 60$ s, $a/R = 1.17$; **c** $t_r = 70$ s, $a/R = 0.95$. *Scale bar* is 100 μm



flowing in the cylindrical pore of channel 5 (Lefebvre et al. 2008; Chu et al. 2011). The method is based on the use of a numerical model of the flow of an initially spherical capsule (radius $a$) in a small cylindrical channel with radius $R$ (Lefebvre et al. 2008; Hu et al. 2012). This model takes into account the fluid–structure interactions which lead to the large deformation (and eventual buckling) of the capsule membrane. As shown recently in our recent study (Hu et al. 2012), it is possible to use an axisymmetric model (Lefebvre et al. 2008), even in the case of large size ratios $a/R$ and membrane buckling. The input parameters of the numerical model are the size ratio $a/R$, the membrane constitutive law and the flow strength normalized by the membrane elastic resistance $\mu Q/\pi R^2 G_s$, where $\mu$ is the external flow viscosity, $Q/\pi R^2$ is the mean flow velocity in the tube and $G_s$ is the surface shear elastic modulus of the capsule membrane. The output of the model is the capsule deformed profile and velocity.

The identification procedure has been described in detail previously (Chu et al. 2011). It consists of determining the deformed capsule profile and velocity inside the cylindrical tube. Note that the leakage flow in the gap around the cylindrical tube has no influence as the measurement is done inside the tube. We then perform contour analysis using the software ImageJ and determine the capsule volume and initial radius $a$ assuming axisymmetry. The contour determination is estimated to lead to a 2 % error on the size ratio. We then characterize the capsule deformation by means of the axial profile length $L$ and the meridional profile area $S$. Assuming that the membrane constitutive law is the neo-Hookean law, we set the value of the size ratio $a/R$ and search a database for the numerical capsule deformed profile with the same values of $L$ and $S$ as the experimental ones. This yields the normalized flow strength and the ratio between the capsule velocity (measured) and the fluid mean velocity. We can then deduce the membrane shear elastic modulus $G_s$.

The values of shear modulus obtained for the three times of cross-linking are indicated in Fig. 6 as a function of the size ratio $a/R$. We find that, for a cross-linking time $t_r = 23$ s, the mean value of the shear modulus is $G_s = 0.004$ N/m with a standard deviation of 0.001 N/m. This value is of the same order as the surface tension between Dragoxat and the HSA solution (0.006 N/m). A cross-linking time of 23 s is therefore too short for a solid membrane to form around the droplet. For the longer cross-linking times, the mean shear modulus of the capsule membrane is found to be $G_s = 0.011 \pm 0.002$ N/m for $t_r = 60$ s, and $G_s = 0.018 \pm 0.002$ N/m for $t_r = 70$ s. These values are significantly larger than the surface tension between Dragoxat and the HSA solution, which confirms that a membrane is formed around the drop, as was already surmised from the observation of wrinkles.

Finally, the evolution of the shear elastic modulus with the cross-linking time is shown in Fig. 7. We find that the shear modulus of the microcapsule membrane increases steeply with the cross-linking time, as was also observed in the case of microcapsules made with an ovalbumin membrane (Chu et al. 2011). The longer the reactants remain in contact, the higher the cross-linking degree in the membranes and then the higher the shear modulus. In addition, this result is in good agreement with our previous findings in bulk emulsion (Edwards-Lévy et al. 1993) showing that for a reaction pH of 9.8, an increase in cross-linking time produced more intensely cross-linked serum albumin microcapsules (less free amino groups, higher ester and anhydride content).

## 4 Discussion

We have designed and used a single microfluidic system to fabricate and directly characterize microcapsule populations. The microdroplet size depends only on the flow rate of the dispersed and continuous phases. The normalized drop length follows the linear regression curve as proposed in the literature (He et al. 2010). However, the slope coefficient is twice that found in our previous work. Various phenomena may account for this discrepancy, such as PDMS swelling when in contact with Dragoxat, the flow rate irregularity of the pump setting and the fuzziness of the droplet image.





Journal : Large 10404 | Dispatch : 4-9-2012 | Pages : 9
Article No. : 1049 | LE | TYPESET
MS Code : mfnf-120507 | CP | DISK

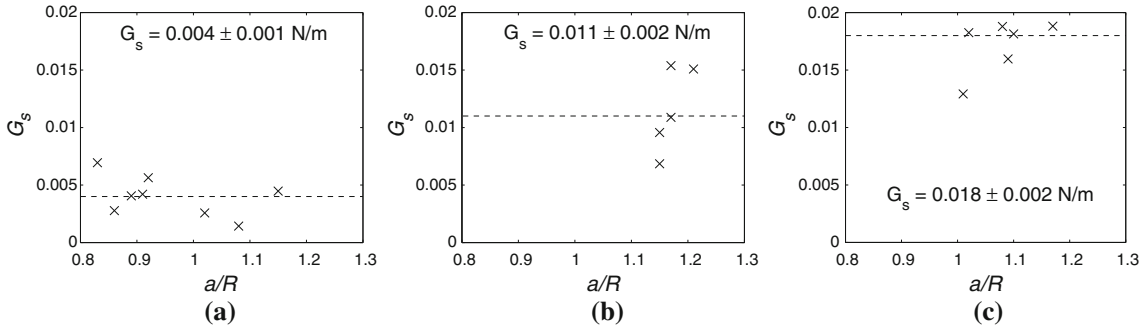


**Fig. 6** Shear modulus of the microcapsule membrane fabricated after **a** 23 s; **b** 60 s; **c** 70 s as a function of the size ratio $a/R$

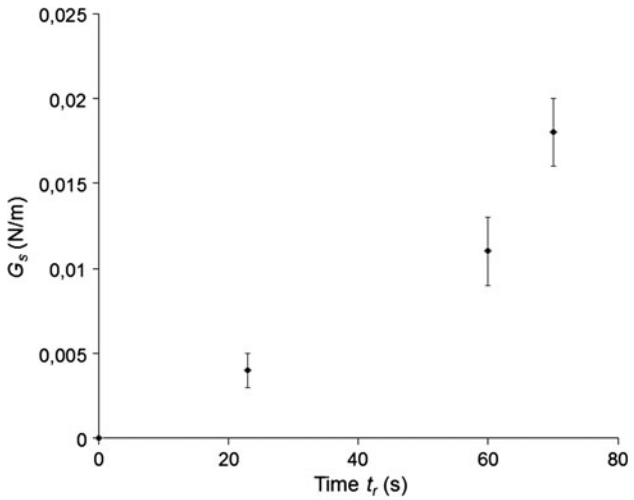


**Fig. 7** Variation of the shear modulus of the albumin membrane of microcapsule as a function of the cross-linking time

The mechanical properties of the microcapsule membrane are characterized with an inverse method. The mean shear modulus of the capsules fabricated after 23 s of cross-linking is of the order of the surface tension between the HSA and Dragoxat solutions: such a low cross-linking time is too short for an elastic membrane to form around the droplet. After 60 s of cross-linking, microcapsules with wrinkles on the membrane are formed. The membrane shear modulus increases when the cross-linking time increases to 70 s. This study shows that the microsystem can be used to combine the fabrication of controlled size microcapsules and their characterization. Indeed, the microfluidic system offers the advantages to fabricate a calibrated capsule population through the formation of droplets of a defined size, followed by a controlled cross-linking reaction. Furthermore, the proposed design enables to measure the geometric and mechanical properties of the capsules using in situ visualizations.

It has not been possible to compare the mechanical properties of serum albumin membrane microcapsules fabricated with the present method (microfluidic technique) and bulk agitation. In bulk agitation, we were not able to collect a stable capsule population below 2 min of cross-linking. For a bulk cross-linking time of 5 min, the serum albumin capsules were stable, but too rigid to be flowed in a microtube and deformed under the hydrodynamic forces. The only points of reference that can be used for comparison are therefore the measurements of populations of microcapsules made with an ovalbumin membrane under bulk agitation. Chu et al. (2011) found that the shear modulus values range from 0.03 to 0.2 N/m according to the pH and the reaction time. Practically, it appears that the present method will not enable the characterization of capsules with a surface shear modulus much larger than 0.2 N/m. Higher shear stresses would need to be generated in the microfluidic channel to deform more rigid microcapsules, but the present setup cannot sustain them. The present measurements have found comparable values (0.011–0.018 N/m for $t_r = 60$–70 s) in the case of serum albumin membrane. It is therefore likely that the microfluidic technique allows for capsule fabrication using short times of cross-linking ($t_r = 60$–70 s), while the conventional technique based on agitation requires a longer time to allow a perfect mixing of the cross-linking solution with the continuous phase of the emulsion (at least $t_r = 5$–30 min). Thus the microfluidic fabrication appears as a new process, which could complement the bulk processes and thus enlarge the spectrum of populations of microcapsules that can be designed and produced.

Despite the fact that the microcapsule populations appear to be stable in the reservoir, we have not yet included protocols to collect and clean the microcapsules. We therefore cannot guarantee their full stability outside the microsystem. This is a key point since the excess of cross-linking agent must be removed to yield a functional capsule population. Another perspective for future development of the microsystem is the insertion of a feedback control on the flow rates of the different phases according to the measured membrane properties. It would enable the optimization of the fabrication conditions on demand.





Journal : Large 10404 Dispatch : 4-9-2012 Pages : 9
Article No. : 1049 LE TYPESET
MS Code : mfnf-120507 CP DISK

## 5 Conclusion

We have proposed a microfluidic device to create and characterize microcapsule populations. The microcapsules are fabricated in a double Y-junction geometry. The shear modulus of the membrane of the microcapsules are obtained from an inverse method coupling experimental and numerical approaches. The numerical model simulates the fluid-structure interactions in the case of a capsule flowing in a cylindrical tube. The microcapsule deformation is measured experimentally in a glass capillary located downstream of the Y-junctions. We then search the numerical database for the parameters that leads to the capsule deformation that is measured and identify them using a best fit method. We presently show that a microcapsule inline fabrication process can be successfully coupled with a characterization method. Setting up a technique to collect and wash the microcapsules will be the next step of our development to propose a functional fabrication process.

**Acknowledgments** This work was supported by the Conseil Regional de Picardie (projects μFIEC and MODCAP).

## References

Andry M-C, Edwards-Lévy F, Lévy M-C (1996) Free amino group content of serum albumin microcapsules III: a study at low pH values. Int J Pharm 128:197–202

Anna SL, Bontoux N, Stone HA (2003) Formation of dispersions using 'flow focusing' in microchannels. Appl Phys Lett 82:364–366

Callewaert M, Millot JM, Lesage J, Laurent-Maquin D, Edwards-Lévy F (2009) Albumin-alginate microspheres: role of structure in binding and release of the krfk peptide. Int J Pharm 366:103–110

Carin M, Barthès-Biesel D, Edwards-Lévy F, Postel C, Andrei DC (2003) Compression of biocompatible liquid-filled HSA-alginate capsules: determination of the membrane mechanical properties. Biotechnol Bioeng 82:207–212

Chu TX, Salsac AV, Leclerc E, Barthès-Biesel D, Wurtz H, Edward-Lévy F (2011) Comparison between measurements of elasticity and free amino group content of ovalbumin microcapsule membranes: discrimination of the cross-linking degree. J Colloid Interf Sci 355:81–88

De Kruif CG, Weinbreck F, De Vries R (2004) Complex coacervation of proteins and anionic polysaccharides. Curr Opin Colloid Interf Sci 9:340–349

Edwards-Lévy F (2011) Microparticulate drug delivery systems based on serum albumin. In: Serum albumin: structure, functions, and health impact. Nova Science

Edwards-Lévy F, Andry M-C, Lévy M-C (1993) Determination of free amino group content of serum albumin microcapsules using trinitrobenzenesulfonic acid: effect of variations in polycondensation pH. Int J Pharm 96:85–90

Edwards-Lévy F, Andry M-C, Lévy M-C (1994) Determination of free amino group content of serum albumin microcapsules: II. Effect of variation time and in terephthaloyl chloride concentration. Int J Pharm 103:253–257

Fery A, Weinkamer R (2007) Mechanical properties of micro and nanocapsules: Single-capsule measurements. Polym Adv Technol 48:7221–7235

Garstecki P, Fuerstman MJ, Stonec HA, Whitesides GM (2006) Formation of droplets and bubbles in a microfluidic T-junction-scaling and mechanism of break-up. Lab Chip 6:437–446

Gautier A, Carpentier B, Dufresne M, Vu Dinh Q, Paulier P, Legallais C (2011) Impact of alginate type and bead diameter on mass transfers and the metabolic activities on encapsulated c3a cells in bioactificial liver applications. Eur Cell Mater 21:94–106

Gibbs BF, Kermasha S, Alli I, Mulligan CN (1999) Encapsulation in the food industry: a review. Int J Food Sc. Nutr 50:213–224

He P, Barthès-Biesel D, Leclerc E (2010) Flow of two immiscible liquids with low viscosity in y shaped microfluidic systems: effect of geometry. Microfluid Nanofluid 9:293–301

Hu X-Q, Salsac A-V, Barthès-Biesel D (2012) Flow of a spherical capsule in a pore with circular or square cross-section. J Fluid Mech (to appear)

Huang K-S, Liu M-K, Wu C-H, Yen Y-T, Lin Y-C (2007) Calcium alginate microcapsule generation on a microfluidic system fabricated using the optical disk process. J Micromech Microeng 17:1428–1434

Hurteaux R, Edwards-Lévy F, Laurent-Maquin D, Lévy M-C (2005) Coating alginate microspheres with a serum albumin-alginate membrane: application to the encapsulation of a peptide. Eur J Pharm Sci 24:187–197

Kissel T, Maretschek S, Packhaser C, Schnieders J, Seidel N (2006) Microencapsulation techniques for parenteral depot systems and their application in the pharmaceutical industry. In: Benita S (ed) Microencapsulation—methods and industrial applications, 2nd edn. Taylor and Francis

Lefebvre Y, Leclerc E, Barthès-Biesel D, Walter J, Edwards-Lévy F (2008) Flow of artificial microcapsules in microfluidic channels: a method for determining the elastic properties of the membrane. Phys Fluids 20:1–10

Lévy MC, Lefebvre S, Rahmouni M, Andry MC, Manfait M (1991) Fourier transform infrared spectroscopic studies of human serum albumin microcapsules prepared by interfacial cross-linking with terephthaloylchloride: Influence of polycondensation ph on spectra and relation with microcapsule morphology and size. J Pharm Sci 80:578–585

Liu L, Yang J-P, Ju X-J, Xie R, Yang L, Liang B, Chu L-Y (2009) Microfluidic preparation of monodisperse ethyl cellulose hollow microcapsules with non-toxic solvent. J Colloids Interf Sci 336:100–106

Mercadé-Prieto R, Zhang Z (2012) Mechanical characterization of microspheres, capsules, cells and beads: a review. J Microencapsulation 29:277–285

Miyazawa K, Yajima I, Kaneda I, Yanaki T (2000) Preparation of a new soft capsule for cosmetics. J Cosmet Sci 51:239–252

Needham D, Zhelev DV (1996) The mechanochemistry of lipid vesicles examined by micropipet manipulation technique. Surf Sci 62:373–444

Ng Lee J, Park C, Whitesides GM (2003) Solvent compatibility of poly(dimethylsiloxane)-based microfluidic devices. Anal Chem 75:6544–6554

Nguyen QT, Bendjama Z, Clment R, Ping Z (1999) Poly(dimethylsiloxane) crosslinked in different conditions. Part I: sorption properties in water-ethyl acetate mixtures. Phys Chem 1:2761–2766

Poux M, Canselier J.P (2004) Techniques et appareillage, procédés d'émulsification. Technique de l'ingénieur, Chapitre 3. J2153. Techniques de l'ingénieur

Sawalha H, Schron K, Boom R (2011) Biodegradable polymeric microcapsules: preparation and properties. Chem Eng J 169: 1–10





Journal : Large 10404 | Dispatch : 4-9-2012 | Pages : 9
Article No. : 1049 | ☐ LE | ☐ TYPESET
MS Code : mfnf-120507 | ☑ CP | ☑ DISK

Thorsen T, Roberts RW, Arnold FH, Quake SR (2001) Dynamic pattern formation in a vesicle-generating microfluidic device. Phys Rev Lett 86:4163–4166

Yeh C-H, Zhao Q, Lee S-J, Lin Y-C (2009) Using a t-junction microdluidic chip for monodisperse calcium alginate mircoparticles and encapsulation of nanoparticles. Sensor Actuat A Phys 151:231–236

Yobas L, Martens S, Ong W-L, Ranganathan N (2006) High-performance flow-focusing geometry for spontaneous generation of monodispersed droplets. Lab Chip 6:1073–1079

Zhang H, Tumarkin E, Peerani R, Nie Z, Sullan RMA, Walker GC, Kumacheva E (2006) Microfluidic production of biopolymer microcapsules with controlled morphology. J Am Chem Soc 128:12205–12210





Journal : Large 10404 | Dispatch : 4-9-2012 | Pages : 9
Article No. : 1049 | ☐ LE | ☐ TYPESET
MS Code : mfnf-120507 | ☑ CP | ☑ DISK